The Journal of Neuroscience, August 1, 1996, *16*(15):4684–4695

Functional GABAergic Synaptic Connection in Neonatal Mouse Barrel Cortex

Ariel Agmon,[1] Greg Hollrigel,[1] and Diane K. O'Dowd[1,2]

Departments of [1]Anatomy and Neurobiology and [2]Developmental and Cell Biology, University of California, Irvine, California 92717

Intracortical inhibition is crucial to proper functioning of the mature neocortex, yet, paradoxically, is reported to be rare or absent in the neonatal animal. We reexamined this issue by recording whole-cell postsynaptic currents (PSCs) of barrel cortex neurons in thalamocortical brain slices from neonatal mice. Monosynaptic, excitatory thalamocortical responses were elicited in layers V/VI neurons as early as postnatal day 0 (P0, the first 24 hr after birth) and in presumptive layer IV as early as P2. At very low stimulation frequencies, the monosynaptic response was invariably followed by a prolonged (up to 1 sec) synaptic barrage, which fatigued at stimulus repetition rates of 2/min or higher. This barrage consisted of postsynaptic responses to spiking activity in neighboring cortical cells, because (1) it could also be evoked by intracortical stimulation in coronal slices and (2) it was abolished by antagonists to NMDA receptors (NMDARs), even when NMDARs on the recorded cell were under a voltage-dependent block. Some of the larger polysynaptic events changed polarity at a negative reversal potential and were blocked by $GABA_A$ receptor ($GABA_AR$) antagonists, with a concurrent enhancement of the extracellular field potential, indicating that they were $GABA_AR$- mediated, Cl-dependent inhibitory PSCs (IPSCs). We conclude that a network of functional intracortical $GABA_AR$-mediated synaptic connections exists from the earliest postnatal ages, although it gives rise to responses that differ from mature IPSCs in reversal potential and latency.

Key words: GABA synapses; synaptic inhibition; postnatal development; barrel cortex; whole-cell recording; synaptic fatigue

GABA-using inhibitory cells comprise, depending on species, 15–25% of the total neuronal population of the mammalian cerebral cortex (Hendry et al., 1987; Meinecke and Peters, 1987; Beaulieu, 1993; Prieto et al., 1994), and their axons give rise to 12–17% of its total number of synaptic contacts (Beaulieu et al., 1992, 1994). This seemingly minor contribution to cortical circuitry belies the vital role of inhibitory synaptic connections in normal cortical function. Loss or impairment of synaptic inhibition in the cerebral or hippocampal cortex is associated with epileptic seizures *in vivo* (Jordan and Jefferys, 1992), and even a slight reduction in efficacy of inhibition results in the emergence of abnormal paroxysmal electrical activity *in vitro* (Chagnac-Amitai and Connors, 1989).

Unlike the situation in the mature cortex, the neonatal cortex is reported to be nearly devoid of structural and functional inhibitory connections. Anatomical studies indicate paucity of axosomatic (putative inhibitory) synaptic contacts in first-week neocortex (Blue and Parnavelas, 1983; Miller, 1986; White et al., 1995). Inhibitory postsynaptic responses to electrical stimulation are absent or rare in upper layers of cat neocortex before postnatal day 30 (P30) (Komatsu and Iwakiri, 1991), in upper layers of rat neocortex before P9 (Luhmann and Prince, 1991; Burgard and Hablitz, 1993), and in layer IV of mouse neocortex before P8 (Agmon and O'Dowd, 1992). Because excitatory synaptic responses to thalamocortical and intracortical stimulation can be elicited in neonatal neocortical neurons (Kriegstein et al., 1987; Agmon and O'Dowd, 1992; Burgard and Hablitz, 1993; Kim et al., 1995), the postulated lack of inhibition implies a gross imbalance between excitation and inhibition in the neonatal cortex, raising the question of why neonatal animals are not in a chronic convulsive state. In the hippocampus, whole-cell recording experiments (Zhang et al., 1991) have challenged earlier studies (Mueller et al., 1984; Swann et al., 1989) that reported late emergence of inhibition in the developing CA1 region of rabbit and rat. Here we report that at very low stimulation frequencies, a thalamocortical volley in P0–8 mice elicited a strong, long-lasting polysynaptic barrage in neurons of cortical layers V/VI and IV. This barrage originated in surrounding cortical cells, and some of its major components were $GABA_A$ receptor ($GABA_AR$)-mediated inhibitory postsynaptic currents (IPSCs).

MATERIALS AND METHODS

Slice preparation and maintenance. Timed pregnant ICR mice dams were monitored at 12 hr intervals to determine time of birth. The first 24 hr after birth were designated P0. Pups were anesthetized by cooling on ice (P4 and younger) or by halothane inhalation (P5 and older) and were decapitated, and the brain was removed into ice-cold artificial cerebrospinal fluid (ACSF) (see below for composition). Brain slices (500 μm thick) were cut on a vibrating tissue slicer in a plane that preserves thalamocortical connectivity (Agmon and Connors, 1991) or in a coronal plane. Two or three slices were transferred to a holding chamber (Edwards and Konnerth, 1992) in which they were submerged in recirculated, oxygenated ACSF at room temperature. After at least 1 hr of incubation, slices were transferred to a submersion recording chamber and superfused continuously at a rate of 2.5–3 ml/min with oxygenated ACSF at room temperature. Transillumination of the slice allowed visual identifi-

Received Feb. 23, 1996; revised May 7, 1996; accepted May 13, 1996.

This work was supported by National Institutes of Health, U.S. Public Health Service, Grant NS30109 to D.K.O'D., with additional support from NS27501 to D.K.O'D. and from NS30109 and NS21377 to E. G. Jones. We thank Drs. Barry Connors, Edward Jones, Yasuo Kawaguchi, Paul Rhodes, and Ivan Soltesz for critical comments on earlier versions of this manuscript.

Correspondence should be sent to Dr. Ariel Agmon's present address: Department of Anatomy, Box 9128, West Virginia University, Morgantown, WV 26506-9128.

cation of many anatomical landmarks, including the ventrobasal complex (VB) and the reticular nucleus of the thalamus (RTN), layer IV of the primary somatosensory cortex, and in favorable preparations, barrels in layer IV (in P4 and older animals) and barreloids within VB (in P2 and older animals). In animals younger than P4, the undifferentiated cortical plate was often recognizable as a dark band immediately below the pial surface. Slices were typically maintained for 12–14 hr after dissection; in one experiment in which the slice was maintained for 26 hr, there was no appreciable deterioration in synaptic responses.

ACSF and drug application. ACSF contained (in mM): 126 NaCl, 3 KCl, 1.25 NaH_2PO_4, 1.3 $MgSO_4$, 2.5 $CaCl_2$, 26 $NaHCO_3$, and 20 dextrose, equilibrated with a 95:5 mixture of O_2/CO_2 to pH 7.4. $CaCl_2$ was added to the solution just before use. Osmolarity of the final solution was 305 ± 5 mOsm. The drugs that were used were D(−)-2-amino-5-phosphonopentanoic acid (APV), 6-cyano-7-nitroquinoxaline-2,3-dione (CNQX), and bicuculline methochloride (BMC), all from RBI (Natick, MA), and they were applied by superfusing the slice with the appropriate concentration of drug dissolved in oxygenated ACSF. When CNQX was used, 1 mM glycine (Sigma, St. Louis, MO) was added to the ACSF.

Whole-cell pipettes and internal solutions. Whole-cell recording pipettes were pulled on a horizontal puller (Sutter Instrument, Novato, CA) from thin-wall, 1.5 mm outer diameter borosilicate glass tubing without filament (WPI, Sarasota, FL) and not modified further. Pipette resistance was typically 10 MΩ (usable range was 5–20 MΩ). Internal solutions were based on either potassium gluconate and cesium gluconate or (in earlier experiments) potassium gluconate and CsF as the main salts, and consisted of (in mM): 130 main salt, 10 KCl, 2 $MgCl_2$, 0.1 $CaCl_2$, 1.1 EGTA, and 10 HEPES. EGTA was dissolved in a measured concentration of KOH, which added 2–4 mM potassium to the final mixture. The solution was titrated with NaOH to pH 7.2–7.4, which added ~4 mM sodium, and its osmolarity was adjusted to 275 ± 5 mOsm, requiring ~5% dilution. Immediately before use, the tip of the pipette was filled by suction with the potassium-based solution. The rest of the pipette was then backfilled with the cesium-based solution, to which were usually added 2–4 mM freshly dissolved potassium ATP (Sigma) and 10 mM QX-314 (RBI).

Electrophysiological recordings and data acquisition. At the start of each experiment, an extracellular field potential pipette (filled with 0.9% NaCl) was placed in layer IV, or in very young animals, in the middle cortical layers. Field potentials were recorded at a gain of 1000× and filtered between 0.1 Hz and 5 KHz. In thalamocortical slices, a tungsten microelectrode (AM Systems, Everett, WA) was placed in VB or at the border of VB and RTN, and 0.1 msec cathodal voltage pulses of increasing intensity were delivered at 30 sec intervals. The positions of the stimulating and recording pipettes were adjusted to achieve the largest amplitude field response to a 5–12 V stimulus (Agmon and Connors, 1991). In very young animals (P0–1), a larger stimulus amplitude (up to 20 V) was sometimes needed to evoke a response. Thalamocortical slices were approached for recording from their anterior face, to maximize the probability of recording responses mediated by orthodromically activated thalamocortical fibers, rather than responses mediated by antidromic activation of corticothalamic axons (Agmon et al., 1993). In coronal slices, the stimulating microelectrode was usually placed in layer VI. "Blind" whole-cell recordings (Blanton et al., 1989), using an Axopatch 1-D amplifier (Axon Instruments, Foster City, CA) with high-frequency cutoff set at 5 kHz, were attempted in either layers V/VI or IV, within ~200 μm on either side of the field potential pipette and up to 150 μm deep in the tissue. When gigaseal was achieved, holding potential was set at −75 mV, and the patch was ruptured by gentle suction. Cells were routinely recorded from for 1–2 hr after break-in, and occasionally for 4 hr or more, with little or no "wash-out" of synaptic responses. Occasionally, resealing of the ruptured patch occurred, which was indicated by a marked decrease in holding current and a reduction in the amplitude of spikes and synaptic responses; in most such cases, reapplication of gentle suction successfully restored the recording.

After the seal was ruptured, current responses to a series of 0.5 sec voltage steps at 10 mV intervals were immediately recorded. These responses, taken before any effects of the backfilled cesium-based QX-314-containing solution were apparent, were used later to determine the resting potential, input resistance, and firing threshold of the cells (see below). Synaptic stimulation was usually initiated at least 20 min after seal rupture to allow for diffusion of the cesium-based solution into the cell. Before this equilibration, current traces recorded during a depolarizing voltage step were noisy and contaminated with spiking activity, and it was not possible to demonstrate reversal of synaptic responses. Extracellular stimuli, at the intensity determined previously when recording the field potential, were delivered with interstimulus intervals of 20–300 sec, and synaptic currents were recorded at several different holding potentials. Extracellular field potential responses were recorded simultaneously with the current responses.

Data were digitized directly and stored in a desktop computer, using the CED data acquisition system (Cambridge, UK). Digital sampling frequency was typically 5 kHz, but for particularly long sweeps, sampling frequency had to be reduced. Stimuli protocols for voltage steps and for synaptic activation were generated using a Master-8 stimulator (AMPI, Jerusalem, Israel).

Junction potential corrections. To correct for junction potentials introduced by our recording solutions, we measured the voltage shift seen by an open-ended pipette when the bath solution was changed from physiological saline to an internal solution (Neher, 1992), using pipettes similar to those used for recording. A patch pipette filled with 3 M KCl was used as an indifferent electrode; voltage shifts were measured in both directions of solution change and averaged from at least three measurements. When measured immediately after backfilling the pipettes, the voltage shifts for CsF- and cesium gluconate-backfilled pipettes were 11 and 12 mV, respectively, when saline was changed to a potassium gluconate-based solution. These values were subtracted *a posteriori* from the holding potentials in the initial voltage-step protocols, because the latter were done immediately after seal rupture, presumably before equilibration of the potassium- and cesium-based solutions inside the pipette, but after at least partial equilibration of the cell interior with the potassium gluconate solution. The average voltage shifts for CsF- and cesium gluconate-backfilled pipettes were 10 and 13 mV, respectively, when saline was changed to the respective cesium-based solution. These measurements were taken at least 10 min after the pipette was filled, to allow for equilibration of solutions inside the pipette, and the recorded voltage shifts were subtracted *a posteriori* from the holding potentials in synaptic response records. Holding potentials labeled in figures are rounded to the nearest 5 mV; however, exact values were used for constructing current–voltage (I–V) curves (see below).

Data analysis. Steady-state current responses to 0.5 sec subthreshold voltage steps were used to construct the I–V relationship of the cell. Input impedance (R_{in}) was calculated as the slope of the I–V curve at −70 mV, measured by fitting a straight line to the three data points straddling the holding potential. Resting potential (V_{rest}) was defined as the voltage at the interpolated intercept of the steady-state I–V curve and the zero current axis. In 21 cells, spiking activity commenced before zero-current level was reached, and in these cases V_{rest} was not defined. All whole-cell current traces shown in this manuscript are single-sweep records, smoothed using a 5-point smoothing algorithm to remove high-frequency noise.

RESULTS

Membrane properties of neonatal cortical cells

The present report is based on whole-cell current records from a sample of 116 neocortical neurons from 34 animals, newborn to 8-d-old. The P0–8 period is defined as "neonatal" for the purpose of this report; it is characterized by a predominantly excitatory short-latency response of layer IV neurons to thalamic stimulation (Agmon and O'Dowd, 1992). The sample was evenly split between layer IV and infragranular (layers V/VI) neurons (layer IV recordings were attempted only in P2 and older preparations). The only criterion for including a cell in the present sample was that the recording lasted long enough for synaptic stimulation to be attempted. All cells were recorded in thalamocortical slices except for 21 cells that were from coronal slices from five animals.

Figure 1 summarizes the resting potentials and input resistances of the cells, grouped according to age and laminar position. There was a distinct difference between layer IV and deep layers neurons. As in CA1 neurons (Spigelman et al., 1992), the median resting potential in deep layers neurons (Fig. 1, *top left*) increased developmentally, from −45 mV in the P0–2 group to −60 mV in the P6–8 group, whereas the median input resistance (Fig. 1, *bottom left*) decreased, from 1.7 GΩ to ~600 MΩ, respectively. In contrast, in layer IV neurons neither electrophysiological parameter displayed any age-dependent change, both being not statisti-

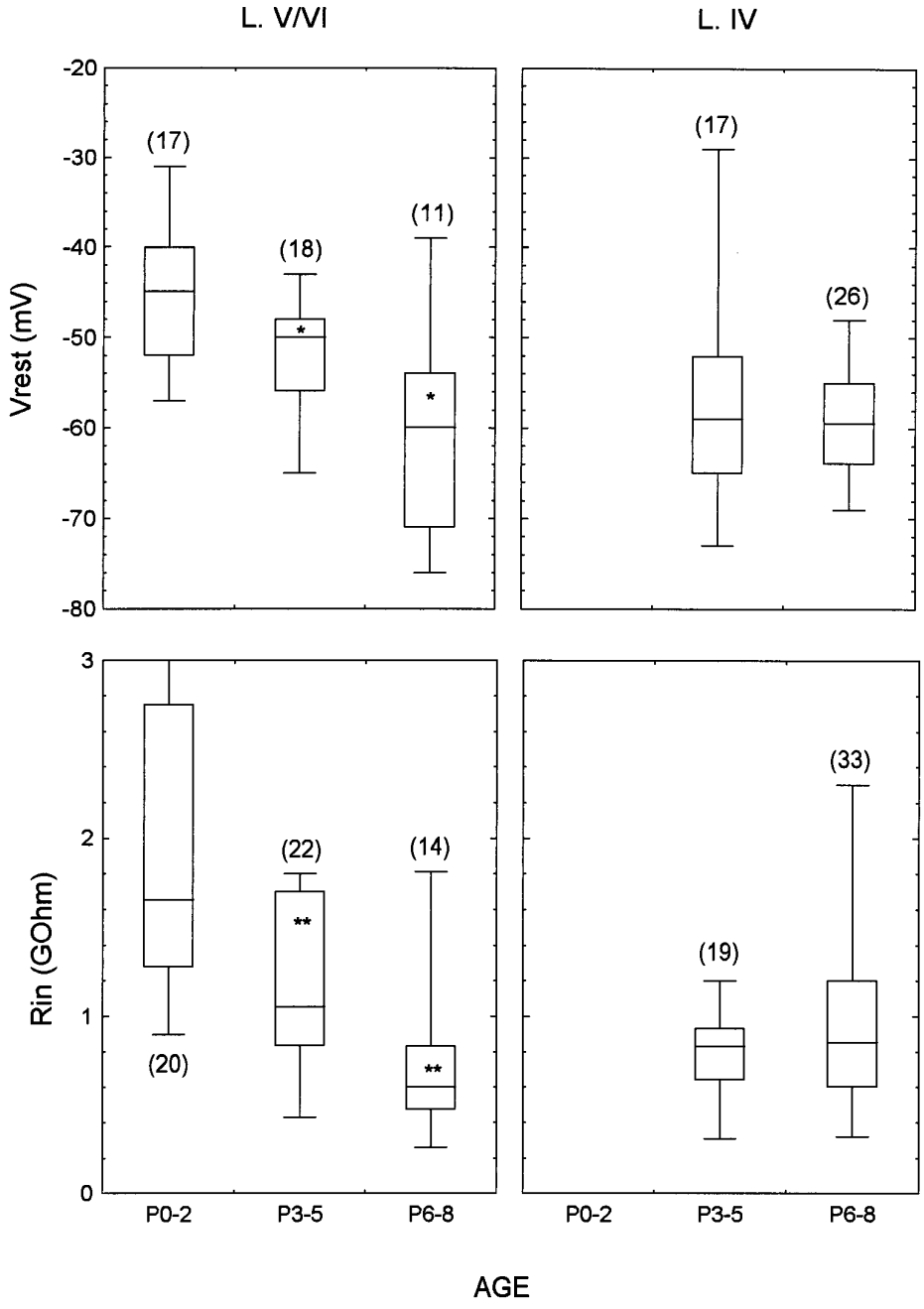

Figure 1. Age-dependent changes in electrophysiological parameters. Resting potentials (*top*) and input resistance (*bottom*) of sampled cells, pooled into three age groups for layers V/VI (*L. V/VI*) cells (*left*), and into two age groups for layer IV (*L. IV*) cells (*right*). (The number of layer IV cells in the youngest age group was too small for analysis.) The *center line* represents the median value; *box* and *whisker lines* represent the 25–75th and 5–95th percentiles, respectively. *Asterisks* denote a statistical significance between one age group and the immediately preceding one, as determined by a two-tailed Mann–Whitney test, with $p < 0.05$ and $p < 0.01$ denoted by *one asterisk* and *two asterisks*, respectively. The number of cells included in each group is indicated in *parentheses*; the discrepancy between the numbers in the upper and lower panels reflects cells for which resting potentials could not be determined, as explained in Materials and Methods.

cally different from the corresponding parameters in P6–8 deep layers neurons (Fig. 1, *right panels*).

Mono- and polysynaptic responses

Neonatal cortical cells exhibited a complex response to a thalamocortical volley. The initial component of the response (Fig. 2, *arrowheads*), exhibited by 82% of layer IV cells and 91% of layers V/VI cells sampled, had a latency of 6–13 msec from stimulus onset (at room temperature) and was identified as monosynaptic by the negligible (<1 msec) trial-to-trial variance in this latency, demonstrated by the superimposed expanded traces in Figure 2*B*. The monosynaptic response was inward-going at all negative holding potentials and often exhibited a nonlinear voltage dependency typical of NMDAR-mediated currents (see Fig. 5*B*, *arrowheads*), consistent with previous pharmacological evidence (Agmon and O'Dowd, 1992). Monosynaptic thalamocortical responses were found in layer IV cells as early as P2, and in layers V/VI cells as early as P0 (not shown), consistent with a recent electron microscopic study demonstrating thalamocortical synapses in deep layers of P0 rat visual cortex (Kageyama and Robertson, 1993).

The monosynaptic response of 94% of all cells that responded monosynaptically to thalamocortical stimulation (including cells as young as P0) was followed by a barrage of long-latency synaptic events (Fig. 2*A*, *asterisks*), in some cases lasting >1 sec (Fig. 3). Two additional cells exhibited a long-lasting barrage that was not preceded by a monosynaptic response (one shown in Fig. 5*A*). As demonstrated by the superimposed traces in Figure 2*B*, there was considerable trial-to-trial variability in the temporal pattern of this barrage as well as its onset (range indicated by *double-sided arrow*), indicating that it was most likely a barrage of polysynaptic

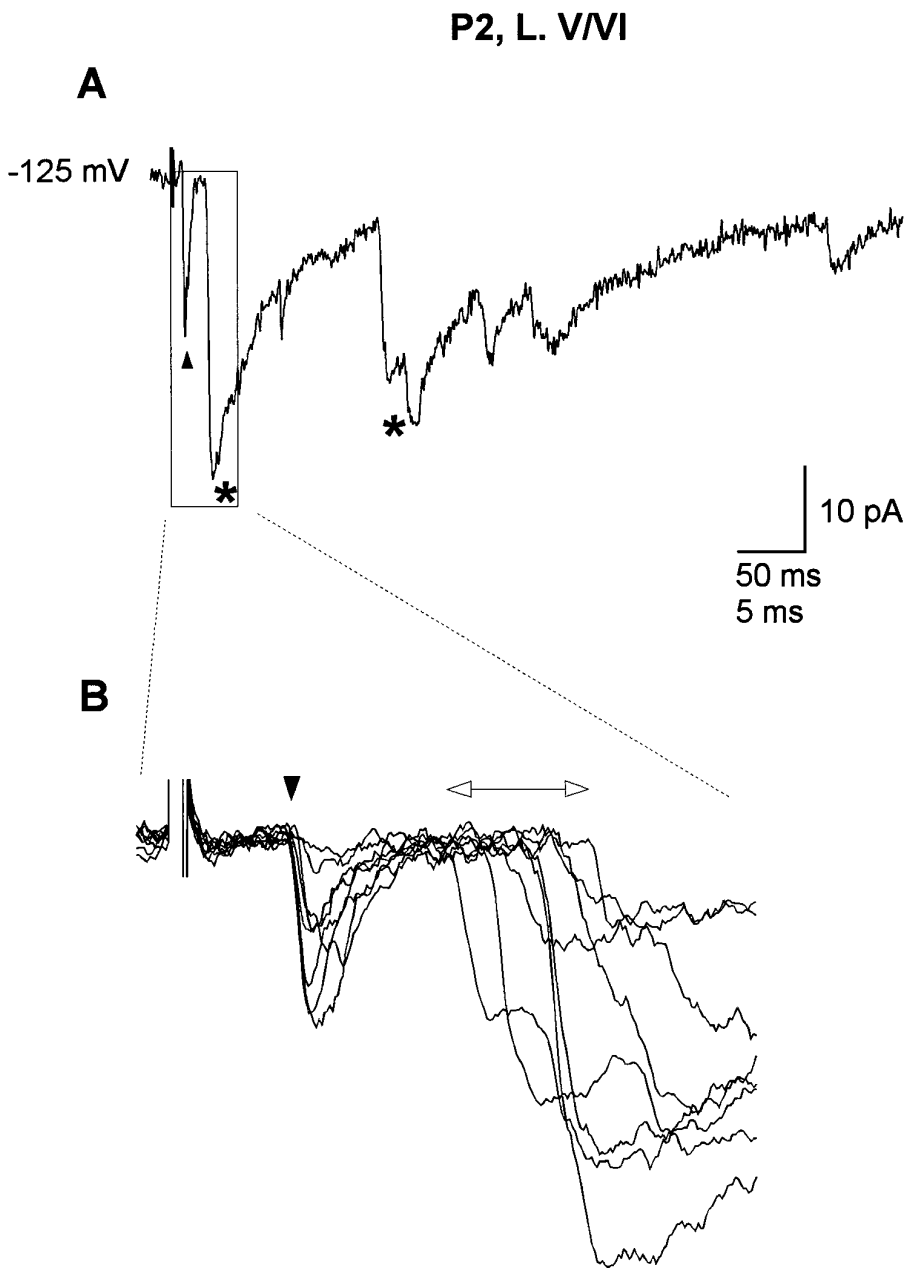

Figure 2. Monosynaptic and polysynaptic components of thalamocortical responses. *A*, Whole-cell postsynaptic current responses of a layer V/VI P2 neuron (*P2, L. V/VI*) to thalamocortical stimulation. Holding potential indicated to the *left* of the trace. The monosynaptic response (its peak marked by *arrowhead*) was followed by a barrage of long-latency events (selected events marked by *asterisks*), in this case lasting >600 msec. *Boxed region* is expanded in *B*. *B*, Superimposed responses to repeated thalamocortical stimulation, at an expanded time base. Compare the small variance in the latency of the monosynaptic component (onset marked by *arrowhead*) with the jitter in the onset of the polysynaptic events (*double arrow*).

events, i.e., synaptic responses to action potentials elicited in surrounding cortical neurons, the latter directly or indirectly activated by the thalamic input. Two alternative interpretations of the prolonged barrage, however, were considered. The first was that it was a monosynaptic response to oscillatory activity in the thalamus, resulting from the reciprocal but inverse connectivity between VB and RTN (Huguenard and Prince, 1994; Warren et al., 1994); the second was that it resulted from a temporally dispersed release of neurotransmitter by immature presynaptic machinery.

To test the first possibility, we recorded postsynaptic responses to intracortical stimulation from 21 neurons (ages P0–7) in coronal slices, which lacked the oscillatory thalamic circuitry. Ninety percent of all cells sampled in coronal slices responded to intracortical stimulation with a prolonged barrage (for examples see Fig. 7), indicating that the barrage originated within the cortex. The second possibility was that the barrage was attributable to temporally dispersed transmitter release from immature thalamocortical axon terminals. Had this been the case, then events in the barrage should have had the same pharmacological sensitivities as monosynaptic thalamocortical responses, i.e., they should have been sensitive to non-NMDA antagonists at all holding potentials, but to NMDA antagonists only at depolarized holding potentials (Agmon and O'Dowd, 1992). As shown in Figure 3, this was not the case. Blocking NMDARs with 12.5 μM APV reversibly and almost totally eliminated the polysynaptic barrage, even at a hyperpolarized holding potential of −130 mV (Fig. 3*A*). Because at this negative voltage, at physiological Mg concentration, the NMDAR channel is fully blocked (Hestrin et al., 1990), the polysynaptic barrage recorded under these conditions could not have been mediated by NMDARs. Its elimination by APV indicated therefore that the synapses blocked by the drug were not located on the cell recorded from but were on unclamped neighboring cortical neurons presynaptic to it. By the same token, the

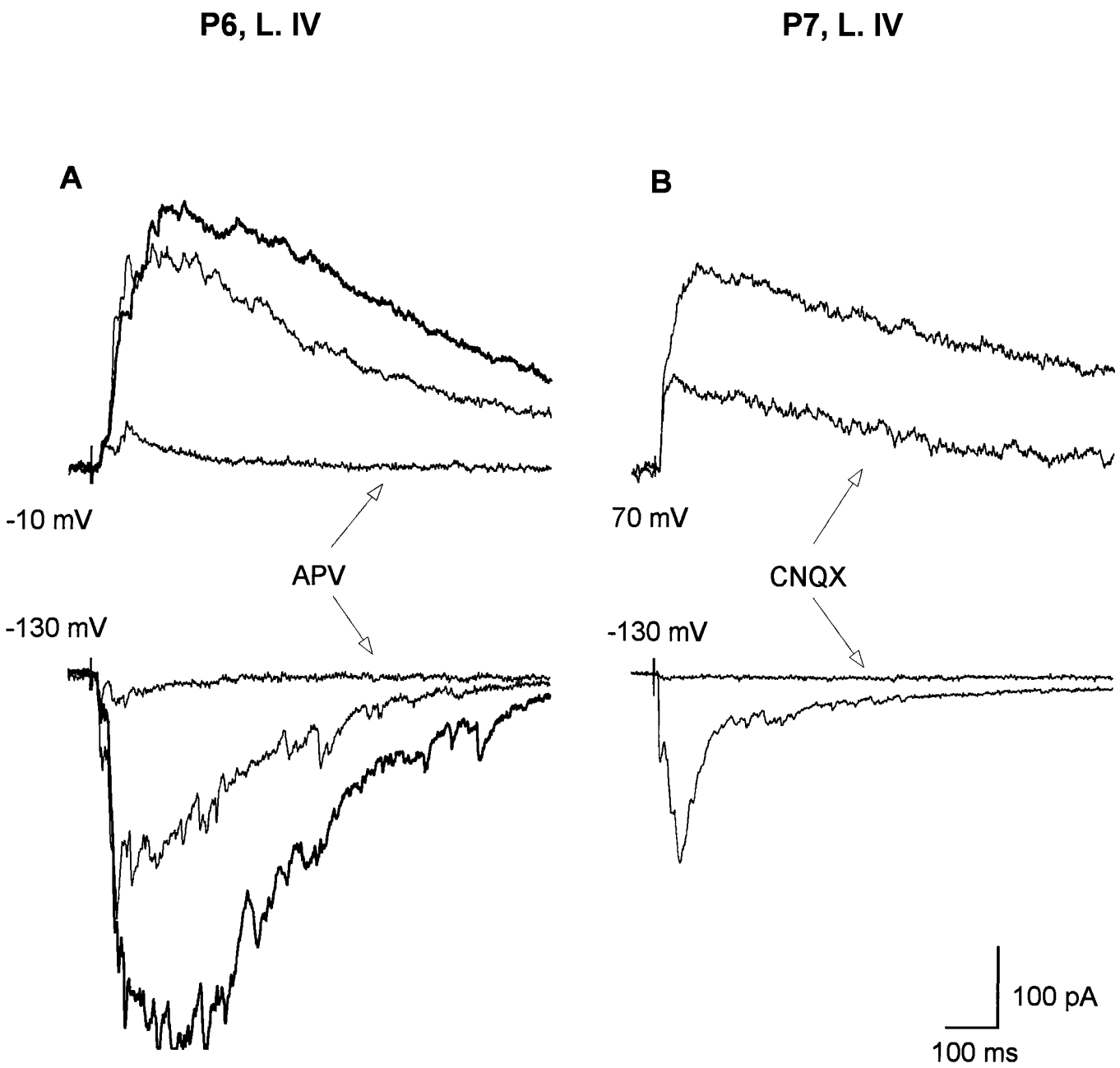

Figure 3. The long-latency PSCs depended on activation of presynaptic neurons through both NMDA and non-NMDA receptors. *A*, Whole-cell currents in response to thalamocortical stimulation of a P6 neuron (*P6, L. IV*), in control ACSF (*light traces*), after addition of 12.5 μM APV (marked by *arrow*) and after drug washout (*heavy traces*). Holding potentials indicated to the *left* of each set of traces. The NMDA antagonist reversibly blocked most of the polysynaptic responses, even at −130 mV, when the response could not have been mediated by NMDA receptors. *B*, Responses of a P7 neuron (*P7, L. IV*) before and after addition of 10 μM CNQX. The non-NMDA antagonist blocked much of the response at +70 mV, even though the late part of this response was probably mediated by NMDA receptors. Both drugs were clearly acting on cells presynaptic to the recorded neurons.

nonlinear voltage dependency of the control response in Figure 3*B* (compare the time course of the response at the depolarized and hyperpolarized potentials) indicated that at least the later part of the response at 70 mV was mediated largely by NMDARs, and therefore the large reduction induced by CNQX indicated that the drug was acting on cells presynaptic to the neuron recorded from. Similar results were achieved in a total of four out of five cells tested (in a fifth cell, 10 μM CNQX reduced the polysynaptic response at a depolarized potential but only delayed the onset of the polysynaptic response at a hyperpolarized potential).

Frequency-dependent fatigue of the polysynaptic barrage

The polysynaptic barrage exhibited a pronounced frequency-dependent fatigue (Fig. 4). At a stimulation rate of 33 mHz (2/min) or higher, consecutive trials elicited an increasingly delayed and shorter barrage, leading to its almost complete failure within two to four trials (Fig. 4*A*). The fatigue was reversible: reducing the rate of stimulation to 5.5 mHz fully restored the response to its previous level at the same stimulation frequency (Fig. 4*B*). Even at 5.5 mHz (i.e., 1/3 per min), however, some

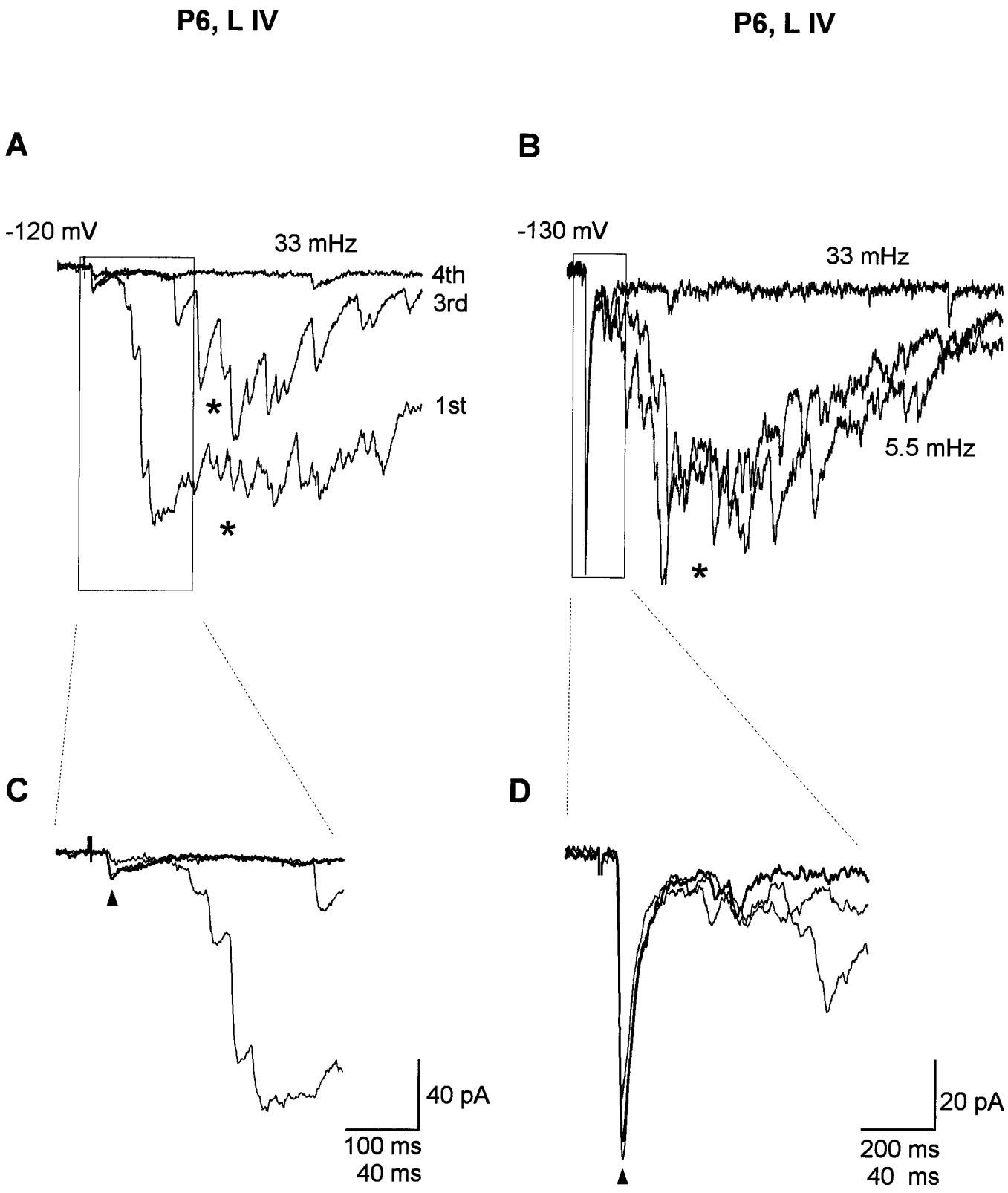

Figure 4. Fatigue of the long-latency responses. Whole-cell postsynaptic responses of two layer IV neurons from different P6 animals (*P6, L IV*). *A*, Superimposed first, third, and fourth responses to thalamocortical stimulation at 33 mHz (2/min); note that the polysynaptic events (*asterisks* in first and third trials) are virtually gone by the fourth repetition of the stimulus. *B*, Representative responses to thalamocortical stimuli from three consecutive trains, delivered at 5.5 mHz and 33 mHz and again at 5.5 mHz. Note the dramatic but reversible fatigue of the polysynaptic responses (*asterisks*) at 33 mHz. The *boxed regions* are expanded in *C* and *D*, showing that the monosynaptic responses (*arrowheads*) were unchanged or even enhanced when the polysynaptic events were maximally fatigued (*heavy line* represents fatigued response).

fatigue was present, because breaks in the stimulation protocol lasting 5 min or more were followed by an even larger response (not shown). At 33 mHz, the monosynaptic response was unchanged or even enhanced (Fig. 4*C,D*, *arrowheads*; the *heavy trace* is the fatigued response); thus the fatigue was not attributable to a reduction in the excitatory drive from the thalamus.

Reversal potentials of the polysynaptic responses

When the membrane potential was clamped at increasingly depolarized voltages, at least some of the larger events comprising the polysynaptic barrage reversed polarity from inward to outward currents (Fig. 5*A,B*, *asterisks*). The reversal occurred at negative holding potentials at which the excitatory, monosynaptic response was still inward-going (Fig. 5*B*, *arrowheads*). To obtain a quantitative estimate of the reversal potential of these PSCs, we chose 12 P3–7 cells, all recorded with cesium gluconate as the main salt and with QX-314 in the pipette, for which it was possible to identify putative unitary PSCs (uPSCs), i.e., responses to individual presynaptic action potentials. We defined putative uPSCs as events with a short (3–5 msec) rising phase lacking any inflection points and followed by an asymptotic decay phase (Fig. 5*A,B*, *asterisks*). There was considerable variability in the sizes of these events in any given trial, probably attributable to variability in neurotransmitter release among different presynaptic axons and during sequential spikes of a single axon. To select a uniform population of uPSCs for reversal potential analysis, we chose from each cell the largest event at each holding potential and plotted its amplitude against the holding potentials. The I–V plots for all 12 cells could be fitted with linear regression lines with a good quality of fit ($r^2 > 0.98$; Fig. 5*C,D*). The slope and zero-intercept of the linear regression line provided an estimate of the synaptic conductance and reversal potential, respectively, of each uPSC. The reversal potentials fell into two nonoverlapping groups (Fig. 6). In the P3–5 age group ($n = 4$), they were -26 ± 2 mV (mean ± SEM), and in the P6–7 age group ($n = 8$) they were -54 ± 3 mV. These differences were highly significant statistically ($p < 0.01$, two-tailed Mann–Whitney test). The difference in the peak conductance of the uPSC (0.7 ± 0.2 nS in the P3–5 cells vs 1.7 ± 0.4 nS in the P6–7 group) was not statistically significant.

To predict the physiological effect of these PSCs on neonatal cortical cells, we compared the reversal potential of the uPSCs, E_{uPSC}, with the resting potential in the same cells, V_{rest}, on a cell-by-cell basis, for three P3–5 and six P6–7 cells for which both quantities were available. In all P3–5 cells, E_{uPSC} was more *positive* than V_{rest} by 12 mV, on average. In five of six P6–7 cells, E_{uPSC} was more *negative* than V_{rest} by 7 mV, on average (in one P7 cell, E_{uPSC} was 7 mV more positive than resting potential). Thus, under physiological conditions, these large synaptic events would be expected to be mostly depolarizing in P5 and younger animals and mostly hyperpolarizing in P6 and older animals.

Pharmacology of the polysynaptic responses

The negative reversal potential of the uPSCs suggested that they were Cl-dependent events activated by GABA. We tested the sensitivity of the neonatal long-latency PSCs to the $GABA_AR$ antagonist BMC (Fig. 7). The drug had a clear effect in five out of six cells from three animals. Of these, in two P3 cells the large polysynaptic events were blocked by BMC, revealing a barrage of small-amplitude events (Fig. 7*A*, *heavy trace*). These small events were presumably glutamate-meditated, although we cannot rule out the possibility that they were GABAergic PSCs, which were only partially blocked by the drug. The monosynaptic excitatory event (Fig. 7*A*, *arrowhead*) was unchanged in BMC, indicating no nonspecific deterioration in preparation viability or recording quality. In three P6–7 cells, application of BMC resulted in an apparently opposite effect, the appearance *de novo* of a large inward synaptic current (Fig. 7*B*, *heavy trace*), suggesting an increased excitability in presynaptic neurons as a result of their release from GABAergic inhibition. In both age groups, but more prominently in the older one, the extracellular record (Fig. 7*C,D*) showed a pronounced and reversible increase in the long-latency negativity in layer IV after BMC application, consistent with disinhibition of the neuronal population.

DISCUSSION

Functional glutamatergic and GABAergic intrinsic connections in neonatal cortex

The major new finding reported here is the existence of functional GABAergic synaptic connections in the neonatal neocortex. These connections were expressed in our experiments as long-lasting polysynaptic barrages triggered by single thalamocortical or intracortical volleys. Long-latency, repetitive synaptic events were reported previously by Kim et al. (1995) in upper cortical layers of neonatal rats, indicating that long-latency barrages in the neonatal cortex are not unique to the mouse or to cortical layers VI–IV. We suggest that the thalamocortical input, mediated by NMDARs and possibly amplified by recurrent excitatory connections, caused a prolonged depolarization of neighboring cortical cells, eliciting in them long trains of action potentials, which through local synaptic connections gave rise to the long-lasting polysynaptic barrages observed in our recordings.

Because both glutamatergic and GABAergic cells were presumably activated by the thalamocortical volley, the polysynaptic barrages probably consisted of both excitatory and inhibitory events. Here we presented direct evidence for inhibitory events. The existence of excitatory synaptic connections in the neonatal neocortex was nevertheless evident in the data demonstrated in Figure 7, in which application of a GABA antagonist gave rise to a large, reversible negativity in the field potential, indicative of a synchronous excitatory response in a large population of neurons and suggesting a recurrent excitatory network unchecked by inhibition. The fact that the whole-cell records showed a large inward current event only in the older animals may indicate that this excitatory network was still underdeveloped in the P3 animals.

Fatigue of polysynaptic barrage

The polysynaptic response was dramatically reduced even at low rates of repetitive stimulation. At the same rates of stimulation, the monosynaptic excitatory response was unaltered, suggesting that the fatigue was not attributable to a reduction in the thalamocortical excitatory drive. More likely, the fatigue was caused by fewer cortical cells firing in response to the same excitatory drive: in other words, by a general reduction in the excitability of the cortical neurons. The cellular mechanism underlying this effect remains to be determined. This fatigability may have contributed to the failure of previous studies to recognize the existence of inhibitory synaptic connections in the neonatal rodent neocortex.

Reversal potential of neonatal uPSCs

Assuming full equilibration between the intracellular milieu and the pipette solution, and assuming a 0.75 coefficient of activity for extracellular Cl (Bormann et al., 1987), the expected Cl reversal potential in our experiments was approximately −50 mV. This is consistent with the observed E_{uPSC}s in the P6 and older cells

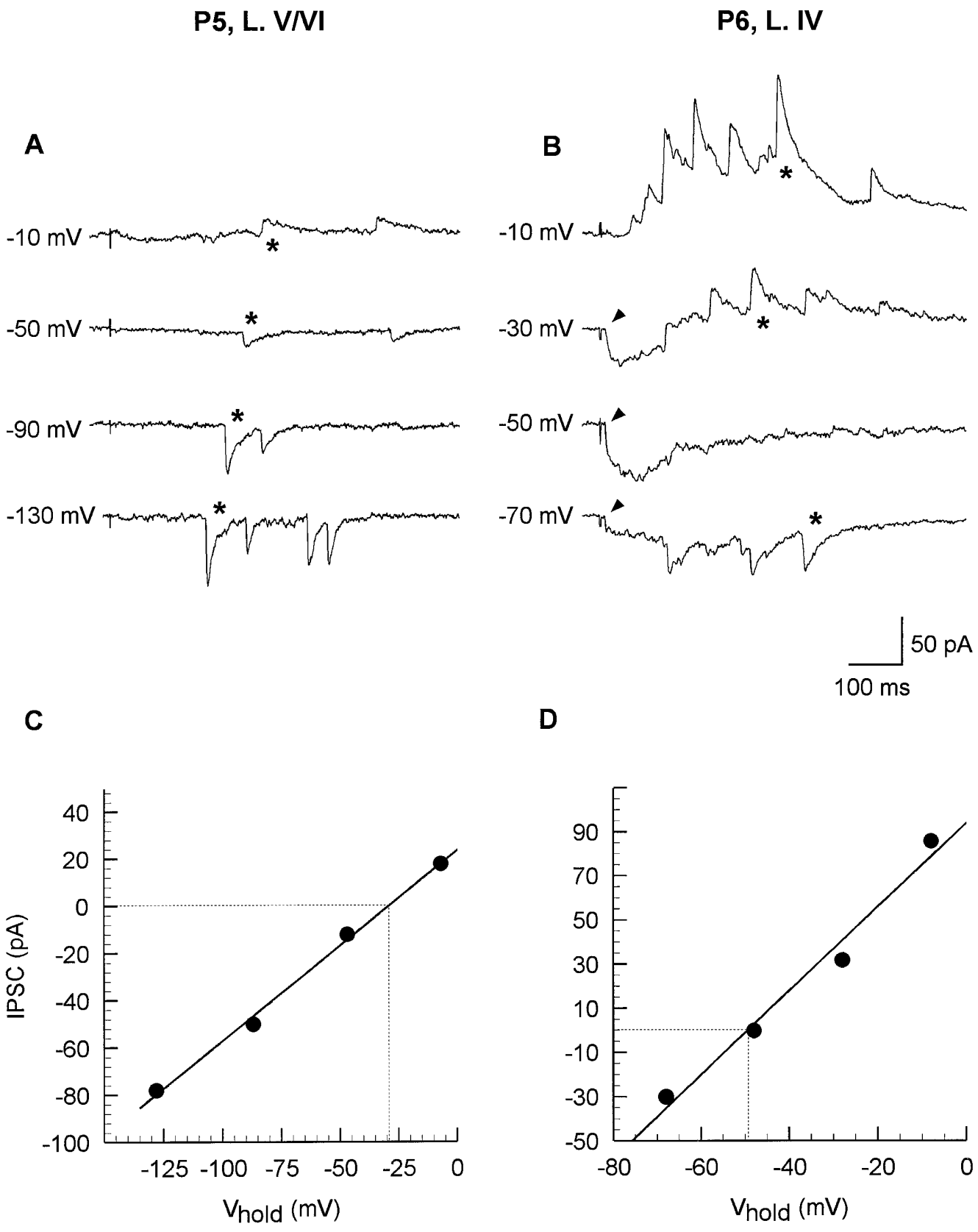

Figure 5. Reversal potentials of unitary polysynaptic events. *A*, Whole-cell postsynaptic currents in a P5 neuron (*P5, L. V/VI*) that exhibited unitary polysynaptic events (largest events marked by *asterisks*) but no monosynaptic response. *B*, Records from a P6 neuron (*P6, L. IV*) that exhibited a monosynaptic response (onset marked by *arrowheads*) followed by a polysynaptic barrage (largest polysynaptic events marked by *asterisks*). The monosynaptic response was inward at all negative potentials and had a voltage dependency characteristic of NMDA receptor-mediated currents. *C*, The largest polysynaptic events in the P5 cell (*asterisks* in *A*) reversed at approximately −30 mV. *D*, The largest polysynaptic events in the P6 cell (*asterisks* in *B*) reversed at approximately −50 mV.

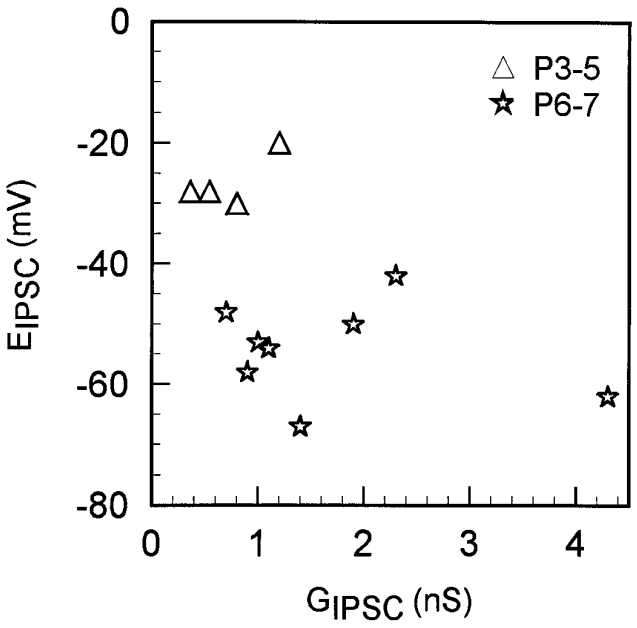

Figure 6. Reversal potentials plotted against synaptic conductance of 12 unitary PSCs. UPSCs in the P3–5 group reversed at or more positive to −30 mV, whereas in the P6–7 group they reversed negative to −40 mV. Synaptic conductances were on average higher (but not significantly so) in the older group as well.

(−54 ± 3 mV), considering that Cl extrusion mechanisms could have contributed to a more negative reversal than expected from passive equilibration alone (Thompson et al., 1988; Zhang et al., 1991). In the P3–5 group, however, E_{uPSC} was nearly 25 mV more *positive* than expected from passive diffusion of Cl. This could be attributable to a Cl *uptake* mechanism in the younger cells (Misgeld et al., 1986; Alvarez-Leefmans, 1990; LoTurco et al., 1995) or, alternatively, to an increased permeability of the synaptic channel in the younger cells to ions with depolarizing reversal potentials. One such ion is the bicarbonate anion, which has a reversal potential near 0 mV (Kaila and Voipio, 1990) and approximately one fifth the permeability of Cl through the GABA-activated channel (Bormann et al., 1987; Kaila et al., 1993). Bicarbonate contributes significantly to $GABA_A$R-mediated responses in neocortex and hippocampus (Kaila et al., 1993; Staley et al., 1995; but see Grover et al., 1993), and indeed a depolarizing reversal potential of $GABA_A$R-mediated responses has also been observed in the neonatal hippocampus (Ben-Ari et al., 1989; Zhang et al., 1991). Because the physiological parameters of the GABA-activated channel depend on its subunit composition (Verdoorn et al., 1990), changes in bicarbonate permeability could arise during development from changes in the relative levels of expression of different $GABA_A$R subunits (Araki et al., 1992; Laurie et al., 1992; Fritschy et al., 1994).

Physiological effect of GABAergic PSCs

The functional effect of a synaptic input depends on its reversal potential relative to spike threshold. In P6 and older preparations, the reversal potential of the uPSCs was more negative than −40 mV, and on a cell-by-cell basis it was almost always more negative than resting potential; therefore, these events were *bona fide* IPSCs. This conclusion is supported by the observation that application of a $GABA_A$R antagonist in P6–7 cells resulted in an appearance *de novo* of a large inward current in the intracellular record (Fig. 7*B*) as well as a large current sink in the extracellular trace (Fig. 7*D*), indicating a disinhibitory effect of the drug (also see Burgard and Hablitz, 1993).

The situation in P5 and younger preparations was somewhat different. In these cases, E_{uPSC} was equal or positive to −30 mV, and on a cell-by-cell basis was always more positive than resting potential and therefore depolarizing. In our sample, however, spike thresholds in the P3–5 age group were significantly higher than in the older age group (our unpublished observations), and therefore E_{uPSC} could have been depolarizing but still below spike threshold and thus inhibitory. In addition, in preparations as young as P3, application of a $GABA_A$R antagonist resulted in enhanced population activity expressed in the evoked field potential (Fig. 7*C*), indicating a disinhibitory effect of the drug and therefore an inhibitory effect of GABA. This result is consistent with the report of induced seizure activity in P3 rats by administration of $GABA_A$R antagonists (Baram and Snead, 1990). Thus it is likely that even in the P3–5 group, the large long-latency PSCs were inhibitory. Although these IPSCs were no doubt less effective than the more hyperpolarizing IPSCs in the older age group, excitatory connections also were probably less developed in the younger animals (see Fig. 7*A* and Discussion above), and thus an overall balance between excitation and inhibition was maintained at both age groups.

Maturation of short-latency intracortical inhibition

In a previous study (Agmon and O'Dowd, 1992), we reported that *short-latency*, thalamocortically evoked responses in P0–8 layer IV neurons are predominantly monosynaptic and excitatory. A short-latency, disynaptic inhibitory response emerges between P8 and P11, when a shift of approximately −60 mV occurs in its reversal potential; this shift was interpreted as a change in the balance between inhibitory and NMDAR-mediated conductances. The shift in reversal potential of the *long-latency* GABAergic PSCs demonstrated in the present study occurred earlier in development and was probably attributable to changes in the anionic selectivity of the $GABA_A$R channel or in the transmembrane Cl gradient. Neither of these changes, however, could account for the shift in *latency* of the IPSCs, from the long latency documented in the present study to the short disynaptic latency of juvenile and mature thalamocortical IPSP/Cs (Agmon and Connors, 1992; Agmon and O'Dowd, 1992). IPSP/C latency depends on the time to spiking of the inhibitory interneuron, which in turn depends on the strength of its excitatory drive and on its integrative properties. It is possible that a large increase in the strength of the thalamocortical input to inhibitory interneurons occurs between P8 and P11. Alternatively or in addition, a negative shift in the firing threshold of inhibitory interneurons could occur, endowing them by the middle of the second postnatal week with the capacity to respond to the thalamocortical input with a short-latency spike. A similar developmental increase in excitability, attributable to an increase in sodium current density and a negative shift in the activation and inactivation curves, has been documented previously in neocortical pyramidal cells (Huguenard et al., 1988; Cummins et al., 1994). Testing these hypotheses would require recording thalamocortical responses from identified inhibitory interneurons in the neonatal cortex.

The role of GABA in the neonatal cortex

A general feature of the embryonic and neonatal CNS is that onset of neurotransmitter synthesis and neurotransmitter receptor expression often precedes the appearance of structural

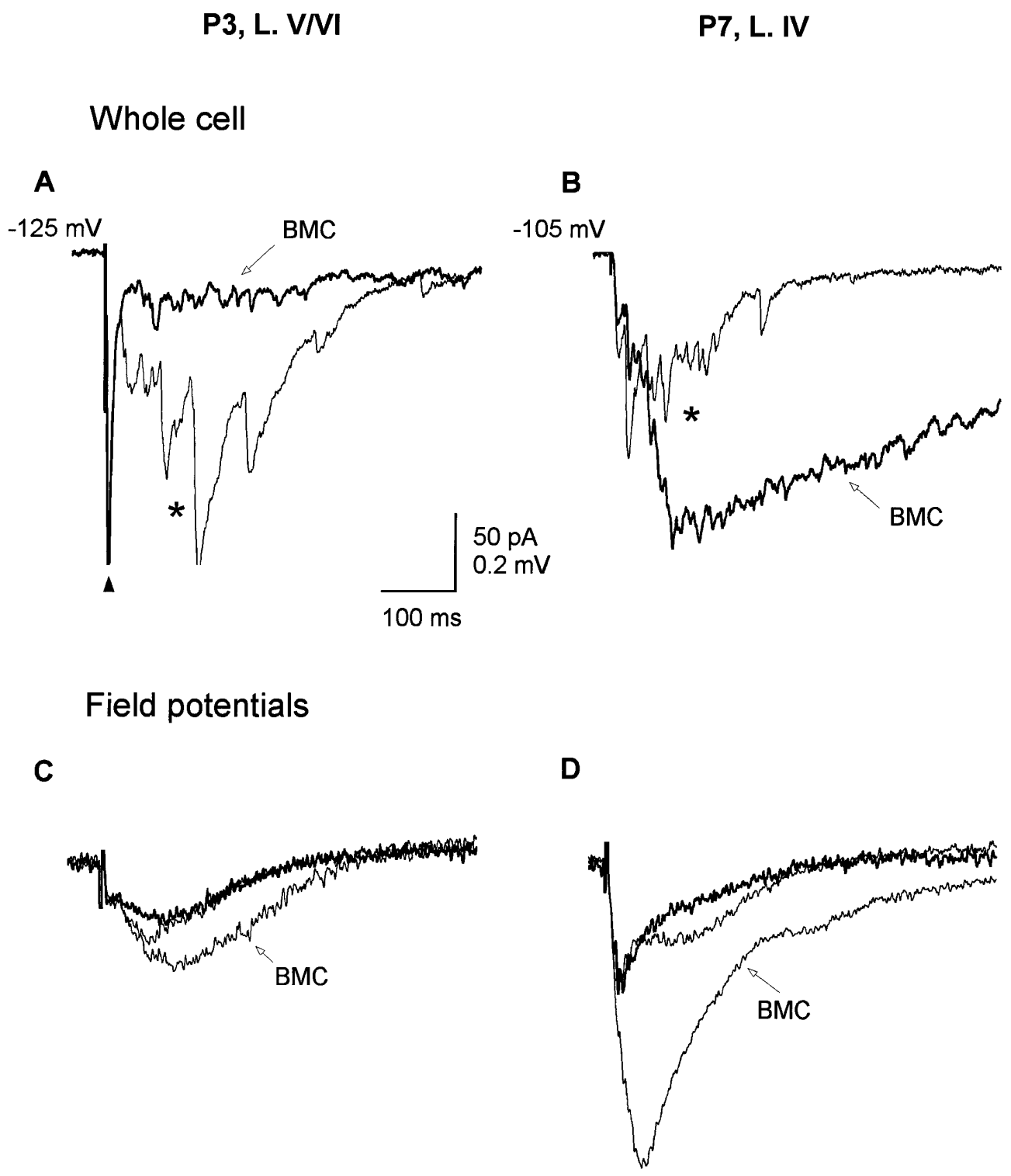

Figure 7. The larger polysynaptic events were GABAergic. *A*, Superimposed whole-cell current responses of a P3 neuron (*P3, L. V/VI*) to intracortical stimulation, in control ACSF (*light trace*) and after addition of 6 μM of the $GABA_AR$ antagonist BMC (*heavy trace*). The polysynaptic events (*asterisk*) were blocked by the drug, revealing a barrage of small, presumably excitatory events. The monosynaptic response (*arrowhead*) was slightly enhanced, indicating no deterioration in the recording. *B*, Postsynaptic currents in a P7 neuron (*P7, L. IV*). Addition of 2 μM BMC (*heavy trace*) caused a *de novo* appearance of inward, presumably excitatory synaptic events (*asterisk*). *C, D*, Averaged field potentials recorded during the experiments shown in *A* and *B*, respectively. *Heavy trace* is the recording taken after drug washout, indicating that the BMC effect was reversible. In both experiments the drug caused a pronounced increase in field potential amplitude, indicating a disinhibitory effect of the drug and therefore an inhibitory effect of GABA.

and functional synaptic connections (Woodward et al., 1971; Blanton and Kriegstein, 1992). This temporal discrepancy has led to the hypothesis that classical neurotransmitters such as GABA and glutamate act during early development in "non-classical" roles of trophic or tropic factors (Behar et al., 1994; LoTurco et al., 1995; for review, see Meier et al., 1991). Our data indicate, however, that a network of functional intracortical GABAergic connections is already in place from the earliest postnatal ages. Thus, in addition to other possible actions, GABA in the neonatal rodent neocortex already functions as a classical neurotransmitter.

REFERENCES

Agmon A, Connors BW (1991) Thalamocortical responses of mouse somatosensory (barrel) cortex in vitro. Neuroscience 41:365–379.

Agmon A, Connors BW (1992) Correlation between intrinsic firing patterns and thalamocortical synaptic responses of neurons in mouse barrel cortex. J Neurosci 12:319–329.

Agmon A, O'Dowd DK (1992) NMDA receptor-mediated currents are prominent in the thalamocortical synaptic response before maturation of inhibition. J Neurophysiol 68:345–349.

Agmon A, Yang LT, O'Dowd DK, Jones EG (1993) Organized growth of thalamocortical axons from the deep tier of terminations into layer IV of mouse barrel cortex. J Neurosci 13:5365–5382.

Alvarez-Leefmans FJ (1990) Intracellular Cl^- regulation and synaptic inhibition in vertebrate and invertebrate neurons. In: Chloride channels and carriers in nerve, muscle and glial cells (Alvarez-Leefmans FJ, Russel JM, eds), pp 109–158. New York: Plenum.

Araki T, Kiyama H, Tohyama M (1992) $GABA_A$ receptor subunit messenger RNAs show differential expression during cortical development in the rat brain. Neuroscience 51:583–591.

Baram TZ, Snead OC (1990) Bicuculline induced seizures in infant rats: ontogeny of behavioral and electrocortical phenomena. Brain Res Dev Brain Res 57:291–295.

Beaulieu C (1993) Numerical data on neocortical neurons in adult rat, with special reference to the GABA population. Brain Res 609:284–292.

Beaulieu C, Kisvarday Z, Somogyi P, Cynader M, Cowey A (1992) Quantitative distribution of GABA-immunopositive and -immunonegative neurons and synapses in the monkey striate cortex (area 17). Cereb Cortex 2:295–309.

Beaulieu C, Campistron G, Crevier C (1994) Quantitative aspects of the GABA circuitry in the primary visual cortex of the adult rat. J Comp Neurol 339:559–572.

Behar TN, Schaffner AE, Colton CA, Somogyi R, Olah Z, Lehel C, Barker JL (1994) GABA-induced chemokinesis and NGF-induced chemotaxis of embryonic spinal cord neurons. J Neurosci 14:29–38.

Ben-Ari Y, Cherubini E, Corradetti R, Gaiarsa JL (1989) Giant synaptic potentials in immature CA3 hippocampal neurones. J Physiol (Lond) 416:303–325.

Blanton MG, Kriegstein AR (1992) Properties of amino acid neurotransmitter receptors of embryonic cortical neurons when activated by exogenous agonist. J Neurophysiol 67:1185–1200.

Blanton MG, LoTurco JJ, Kriegstein AR (1989) Whole cell recording from neurons in slices of reptilian and mammalian cerebral cortex. J Neurosci Methods 30:203–210.

Blue ME, Parnavelas JG (1983) The formation and maturation of synapses in the visual cortex of the rat. II. Quantitative analysis. J Neurocytol 12:697–712.

Bormann J, Hamill OP, Sakmann B (1987) Mechanism of anion permeation through channels gated by glycine and γ-aminobutyric acid in mouse cultured spinal neurones. J Physiol (Lond) 385:243–286.

Burgard EC, Hablitz JJ (1993) Developmental changes in NMDA and non-NMDA receptor-mediated synaptic potentials in rat neocortex. J Neurophysiol 69:230–240.

Chagnac-Amitai Y, Connors BW (1989) Horizontal spread of synchronized activity in neocortex and its control by GABA-mediated inhibition. J Neurophysiol 61:747–758.

Cummins TR, Xia Y, Haddad GG (1994) Functional properties of rat and human neocortical voltage-sensitive sodium currents. J Neurophysiol 71:1052–1064.

Edwards FA, Konnerth A (1992) Patch-clamping cells in sliced tissue preparations. In: Methods in enzymology, Vol 207 (Rudy B, Iverson LE, eds), pp 208–222. San Diego: Academic.

Fritschy JM, Paysan J, Enna A, Mohler H (1994) Switch in the expression of rat $GABA_A$-receptor subtypes during postnatal development: an immunohistochemical study. J Neurosci 14:5302–5324.

Grover LM, Lambert NA, Schwartzkroin PA, Teyler TJ (1993) Role of HCO_3^- ions in depolarizing $GABA_A$ receptor-mediated responses in pyramidal cells of rat hippocampus. J Neurophysiol 69:1541–1555.

Hendry SH, Schwark HD, Jones EG, Yan J (1987) Numbers and proportions of GABA-immunoreactive neurons in different areas of monkey cerebral cortex. J Neurosci 7:1503–1519.

Hestrin S, Nicoll RA, Perkel DJ, Sah P (1990) Analysis of excitatory synaptic action in pyramidal cells using whole-cell recording from rat hippocampal slices. J Physiol (Lond) 422:203–225.

Huguenard JR, Prince DA (1994) Intrathalamic rhythmicity studied in vitro: nominal T-current modulation causes robust antioscillatory effects. J Neurosci 14:5485–5502.

Huguenard JR, Hamill OP, Prince DA (1988) Developmental changes in Na^+ conductances in rat neocortical neurons: appearance of a slowly inactivating component. J Neurophysiol 59:778–795.

Jordan SJ, Jefferys JG (1992) Sustained and selective block of IPSPs in brain slices from rats made epileptic by intrahippocampal tetanus toxin. Epilepsy Res 11:119–129.

Kageyama GH, Robertson RT (1993) Development of geniculocortical projections to visual cortex in rat: evidence for early ingrowth and synaptogenesis. J Comp Neurol 335:123–148.

Kaila K, Voipio J (1990) GABA-activated bicarbonate conductance: influence on E_{GABA} and on postsynaptic pH regulation. In: Chloride channels and carriers in nerve, muscle and glial cells (Alvarez-Leefmans FJ, Russel JM, eds), pp 331–352. New York: Plenum.

Kaila K, Voipio J, Paalasmaa P, Pasternack M, Deisz RA (1993) The role of bicarbonate in $GABA_A$ receptor-mediated IPSPs of rat neocortical neurones. J Physiol (Lond) 464:273–289.

Kim HG, Fox K, Connors BW (1995) Properties of excitatory synaptic events in neurons of primary somatosensory cortex of neonatal rats. Cereb Cortex 5:148–157.

Komatsu Y, Iwakiri M (1991) Postnatal development of neuronal connections in cat visual cortex studied by intracellular recording in slice preparation. Brain Res 540:14–24.

Kriegstein AR, Suppes T, Prince DA (1987) Cellular and synaptic physiology and epileptogenesis of developing rat neocortical neurons in vitro. Brain Res 431:161–171.

Laurie DJ, Wisden W, Seeburg PH (1992) The distribution of thirteen $GABA_A$ receptor subunit mRNAs in the rat brain. III. Embryonic and postnatal development. J Neurosci 12:4151–4172.

LoTurco JJ, Owens DF, Heath MJS, Davis MBE, Kriegstein AR (1995) GABA and glutamate depolarize cortical progenitor cells and inhibit DNA synthesis. Neuron 15:1287–1298.

Luhmann HJ, Prince DA (1991) Postnatal maturation of the GABAergic system in rat neocortex. J Neurophysiol 65:247–263.

Meier E, Hertz L, Schousboe A (1991) Neurotransmitters as developmental signals. Neurochem Int 19:1–15.

Meinecke DL, Peters A (1987) GABA immunoreactive neurons in rat visual cortex. J Comp Neurol 261:388–404.

Miller MW (1986) Maturation of rat visual cortex. III. Postnatal morphogenesis and synaptogenesis of local circuit neurons. Brain Res 390:271–285.

Misgeld U, Deisz RA, Dodt HU, Lux HD (1986) The role of chloride transport in postsynaptic inhibition of hippocampal neurons. Science 232:1413–1415.

Mueller AL, Taube JS, Schwartzkroin PA (1984) Development of hyperpolarizing inhibitory postsynaptic potentials and hyperpolarizing response to gamma-aminobutyric acid in rabbit hippocampus studied in vitro. J Neurosci 4:860–867.

Neher E (1992) Correction for liquid junction potentials in patch clamp experiments. In: Methods in enzymology, Vol 207 (Rudy B, Iverson LE, eds), pp 123–131. San Diego: Academic.

Prieto JJ, Peterson BA, Winer JA (1994) Morphology and spatial distribution of GABAergic neurons in cat primary auditory cortex (AI). J Comp Neurol 344:349–382.

Spigelman I, Zhang L, Carlen PL (1992) Patch-clamp study of postnatal development of CA1 neurons in rat hippocampal slices: membrane excitability and K^+ currents. J Neurophysiol 68:55–69.

Staley KJ, Soldo BL, Proctor WR (1995) Ionic mechanisms of neuronal excitation by inhibitory $GABA_A$ receptors. Science 269:977–981.

Swann JW, Brady RJ, Martin DL (1989) Postnatal development of GABA-mediated synaptic inhibition in rat hippocampus. Neuroscience 28:551–561.

Thompson SM, Deisz RA, Prince DA (1988) Relative contributions of passive equilibrium and active transport to the distribution of chloride in mammalian cortical neurons. J Neurophysiol 60:105–124.

Verdoorn TA, Draguhn A, Ymer S, Seeburg PH, Sakmann B (1990) Functional properties of recombinant rat $GABA_A$ receptors depend upon subunit composition. Neuron 4:919–928.

Warren RA, Agmon A, Jones EG (1994) Oscillatory synaptic interactions between ventroposterior and reticular neurons in mouse thalamus in vitro. J Neurophysiol 72:1993–2003.

White EL, Lev D, Weinfeld E (1995) The development of synapses in barrels of mouse primary somatosensory cortex. Soc Neurosci Abstr 21:1777.

Woodward DJ, Hoffer BJ, Siggins GR, Bloom FE (1971) The ontogenic development of synaptic functions, synaptic activation and responsiveness to neurotransmitter substances in rat cerebellar Purkinje cells. Brain Res 34:75–97.

Zhang L, Spigelman I, Carlen PL (1991) Development of GABA-mediated, chloride-dependent inhibition in CA1 pyramidal neurones of immature rat hippocampal slices. J Physiol (Lond) 444:25–49.